

Studies of waveform requirements for intermediate mass-ratio coalescence searches with advanced gravitational-wave detectors

R. J. E. Smith,^{1,2} I. Mandel,¹ and A. Vecchio¹

¹*School of Physics and Astronomy, University of Birmingham, Edgbaston, Birmingham B15 2TT, UK*

²*Perimeter Institute for Theoretical Physics, Waterloo, Ontario N2L 2Y5, Canada*

The coalescence of a stellar-mass compact object into an intermediate-mass black hole (intermediate mass-ratio coalescence; IMRAC) is an important astrophysical source for ground-based gravitational-wave interferometers in the so-called advanced (or second-generation) configuration. However, the ability to carry out effective matched-filter based searches for these systems is limited by the lack of reliable waveforms. Here we consider binaries in which the intermediate-mass black hole has mass in the range $24 M_{\odot} - 200 M_{\odot}$ with a stellar-mass companion having masses in the range $1.4 M_{\odot} - 18.5 M_{\odot}$. In addition, we constrain the mass ratios, q , of the binaries to be in the range $1/140 \leq q \leq 1/10$ and we restrict our study to the case of circular binaries with non-spinning components. We investigate the relative contribution to the signal-to-noise ratio (SNR) of the three different phases of the coalescence: inspiral, merger and ringdown using waveforms computed within the effective one-body formalism matched to numerical relativity, known as EOBNR. We show that merger and ringdown contribute to a substantial fraction of the total SNR over a large portion of the mass parameter space, although in a limited portion the SNR is dominated by the inspiral phase. We further identify three regions in the IMRAC mass-space in which: (i) inspiral-only searches could be performed with losses in detection rates L in the range $10\% \lesssim L \lesssim 27\%$, (ii) searches based on inspiral-only templates lead to a loss in detection rates in the range $27\% \lesssim L \lesssim 50\%$, and (iii) templates that include merger and ringdown are essential to prevent losses in detection rates greater than 50%. In addition we find that using inspiral-only templates as filters can lead to large biases in the estimates of the mass parameters of IMRACs. We investigate the effectiveness with which the inspiral-only portion of the IMRAC waveform space is covered by comparing several existing waveform families in this regime. We find that different waveform families are only marginally effective at describing one another, as measured by the ‘‘fitting factor’’. Our results reinforce the importance of extensive numerical relativity simulations of IMRACs to validate and calibrate semi-analytical waveform families and the need for further studies of suitable approximation schemes in this mass range.

I. INTRODUCTION

Observations of ultra-luminous X-ray sources and simulations of globular cluster dynamics suggest the existence of intermediate-mass black holes (IMBHs). However, observational evidence for their existence is still under debate, see e.g. [1, 2]. Gravitational waves from binary coalescences involving IMBHs with masses $50 M_{\odot} \lesssim M \lesssim 500 M_{\odot}$ are potentially detectable by advanced detectors – including Advanced LIGO [3], Advanced Virgo [4], and KAGRA [5] – with a low frequency cutoff of around 10 Hz. If IMBHs do exist, one likely contribution to gravitational-wave detections is believed to be through the coalescence of a compact stellar-mass companion (black hole or neutron star) with an IMBH, at a possible rate of up to $\sim 10 \text{ yr}^{-1}$ [6–8]. We will denote these signals as intermediate mass-ratio coalescences (IMRACs)¹.

Given that IMBHs in this mass range have proved extremely difficult to observe in the electromagnetic spectrum, gravitational-wave detections may provide the first unambiguous observations of such objects through the robust measurement of their masses. Such observations would form an important channel for probing the dynamical history of globular clusters. Furthermore, Advanced LIGO/Virgo (aLIGO/Virgo) may be able to provide measurements of the quadrupole moment of a black hole [7, 9], which would allow a null-hypothesis test of the Kerr metric for IMBHs.

The gravitational waveform from the coalescence of two compact objects can be divided into three phases: a gradual inspiral, a rapid merger, and the quasi-normal ringdown of the resulting black hole. The relative contribution to the expected coalescence signal from inspiral, merger and ringdown is an important consideration for gravitational-wave searches. To leading Newtonian order the gravitational wave frequency at the inner-most stable circular orbit (ISCO) is

$$f_{\text{ISCO}} = 4.4 \text{ kHz} \left(\frac{M_{\odot}}{M} \right), \quad (1.1)$$

where M is the total mass of the binary. For advanced detectors with a low frequency cut-off of ~ 10 Hz, we may only have access to either the very late stages of the

¹ In the literature, the term frequently used for this class of objects is *intermediate mass-ratio inspirals* or IMRIs, see e.g. [7, 8]. However, in the context of ground-based observations, in particular with second-generation instruments, we will show that the full coalescence is important for these systems, and it therefore seems to be more appropriate to call them IMRAC.

inspiral, or solely merger and ringdown for the heaviest IMRAC systems. While the power in the merger and ringdown is suppressed by a factor of the mass ratio relative to the power in the inspiral, the fact that IMRAC systems are liable to merge either in-band, or at the low frequency limit of the bandwidth, means that merger and ringdown may be significant over a large portion of the detectable mass-space. Additionally, for cases where IMRAC waveforms are inspiral-dominated, it is useful to know where inspiral-only searches could be targeted.

Detecting IMRACs through gravitational waves will require template gravitational-waveform families adapted to highly asymmetrical mass-ratio systems. However the development of numerical relativity simulations and perturbative techniques in this regime is at an early stage which is potentially problematic (see, e.g. [10] for a discussion of this issue). The issue of appropriate template waveform families is thus central to the detection of IMRACs through gravitational waves.

The effective-one-body approach, calibrated to numerical relativity, has led to template waveforms, known as EOBNR [11], that describe the full inspiral, merger and ringdown coalescence-signal for comparable mass-ratio binaries; EOBNR waveforms should also be accurate at extreme mass ratios. However, to date only one full numerical simulation exists for mass-ratio $q = 1/100$ binaries [12]. Furthermore, EOBNR waveforms have been constructed to reproduce the dynamical evolution of binaries with extreme mass ratios. EOBNR waveforms have not yet been compared to numerical relativity simulations at such mass ratios, so their validity in the IMRAC regime remains to be demonstrated.

Meanwhile, in the context of extreme mass-ratio binaries, several authors have modelled the two-body motion by computing radiative and conservative self-force corrections to Kerr geodesic motion [13, 14]. Waveforms computed within this scheme are inspiral-only and are only developed to lowest order in the mass ratio. These waveforms have been adapted to describe intermediate mass-ratio inspirals by including higher-order-in-mass-ratio corrections in [15] and have been used to study the detection of intermediate mass-ratio inspirals in the context of the proposed third-generation ground-based gravitational-wave interferometer the Einstein Telescope [16]. We refer to these intermediate mass-ratio inspiral waveforms as the ‘‘Huerta Gair’’ (HG) waveform family after its authors. This waveform family should be physically well motivated to describe the inspiral of IMRACs.

Typically one does not have an exact representation of ‘‘true’’ gravitational-wave signals but requires templates which are sufficiently effective at filtering such signals. A common metric for quantifying how well approximate waveform families are at filtering gravitational-wave signals is known the ‘‘effectiveness’’, or fitting factor [17]. This measures the fraction of the theoretical maximum signal-to-noise ratio (SNR) that could be recovered by using non-exact template waveforms.

The work in this paper proceeds as follows. Firstly,

by computing the effectiveness of inspiral-only template waveforms at filtering the full coalescence signal, we determine the relative importance of the inspiral and merger-ringdown phases. We identify three regions in the component mass plane in which: (a) inspiral-only searches are feasible with losses in detection rates L in the range $10\% \lesssim L \lesssim 27\%$, (b) searches are limited by the lack of merger and ringdown in template waveforms and are liable to incur losses in detection rates in the range $27\% \lesssim L \lesssim 50\%$, and (c) merger and ringdown are essential for searches in order to prevent losses in detection rates greater than 50%. We also study the biases incurred in estimates of the mass parameters of IMRACs when using inspiral-only waveforms to filter signals which are described by full inspiral, merger and ringdown waveforms. We find that estimates in the chirp mass and symmetric mass ratio of IMRACs can be biased by as much as 50% and 160%, respectively, of the values encoded in the signal waveform.

Secondly, to gain insight into the accuracy of the inspiral portion of IMRAC waveforms we compute the effectiveness of the inspiral-only portion of EOBNR waveforms at filtering gravitational-wave signals as described by the HG waveform family. We find that there is a non-negligible discrepancy between EOBNR and HG inspirals in the regime where inspiral-only searches could be considered sufficient. For reference we also compare EOBNR inspirals to a post-Newtonian (PN) waveform family known as TaylorT4 [17]. The PN expansion is liable to be a poor choice of approximant for IMRACs because of the large number of cycles spent at small radii. We find that EOBNR and HG are in better agreement with each other than to TaylorT4, as might be expected from the previous observation.

Our approach does not directly address the accuracy of template waveforms, because none of the waveforms considered have been matched to full numerical waveforms. However, assuming that the waveform families we consider ‘‘bracket’’ the correct gravitational waveforms in the IMRAC regime, this approach provides a useful heuristic for quantifying the effectiveness of existing gravitational waveforms for IMRAC searches. Further numerical relativity simulations will be important in the continuing development of accurate template waveforms for IMRACs.

Our analysis improves upon previous work to determine the detectability of IMRAC sources [18] which only considered the so-called ‘‘faithfulness’’ of template waveforms, i.e., the effectiveness of template waveforms evaluated at the signal parameters. Additionally, that study only considered inspiral-only waveforms and focused on low frequency observations, e.g. with the proposed Laser Interferometer Space Antenna (LISA).

This paper is organized as follows. In Sec. II we describe the waveform families used in our study. In Sec. III we compute the contributions to the SNR from the inspiral and merger and ringdown phases of EOBNR waveforms in the intermediate mass-ratio regime. In Sec. IV we study the effectiveness of inspiral-only waveforms to

filter full coalescence signals from IMRAC sources and identify the three regions in which different searches could be conducted. In Sec. IV A we study biases incurred in estimates of the mass parameters of IMRAC sources through using inspiral-only templates to filter full inspiral, merger and ring-down waveforms. In Sec. V we compare the inspiral portion of EOBNR waveforms to HG and TaylorT4 waveforms. In Sec VI we consider the implications of our results for future searches in advanced detectors.

II. WAVEFORMS

In this section we summarise the key concepts entering the construction of the waveforms used in this study. Throughout the paper, for a binary system with individual component masses m_1 and m_2 (with $m_2 < m_1$) we define the total mass as $M \equiv m_1 + m_2$, and mass ratio and symmetric mass ratio as $q \equiv m_2/m_1$ and $\eta \equiv m_1 m_2 / (m_1 + m_2)^2$, respectively.

We consider the family of waveforms constructed by calibrating the effective-one-body approach to numerical relativity (EOBNR) [11]. The EOBNR family describes the full inspiral-merger-ringdown signal; it is currently used in searches that reach the IMBH mass range, so far up to $100 M_\odot$ [19]. The free parameters in the family have been fitted to comparable mass ratio numerical relativity simulations, and by construction this family is deemed to be faithful in the test particle limit. For this work, we use the implementation provided by the LIGO Scientific Collaboration Algorithm Library (LAL) that corresponds to the approximant EOBNRv2.

We also consider a waveform family based on test particle motion in Kerr/Schwarzschild space-time with radiative and conservative self-force corrections which we refer to as the Huerta-Gair (HG) family [16]. The approximation scheme is constructed specifically to handle highly-asymmetrical mass-ratio binaries and is therefore a physically well motivated approximation scheme for intermediate mass-ratio inspirals. These waveforms have been compared against, Teukolsky based waveforms for inspiralling test particles on geodesic orbits and the match exceeds 95% over a large portion of the parameter space [15]. These waveforms have been used to study the detection of intermediate mass-ratio inspirals by the Einstein Telescope in [16]. The Huerta-Gair waveforms describe only the inspiral portion of the coalescence signal. There is no corresponding LAL approximant. The gravitational-wave polarization states can be computed from Eqs. (14) and (15) of [16]. For our study, effects of orientation of the gravitational-wave source are irrelevant and we can consider only circularly-polarized face-on binaries. We fix the spin parameter to zero.

Finally, as a reference we use the standard inspiral-only post-Newtonian approximation corresponding to the LAL approximant TaylorT4, which includes corrections to the phase of the waveform at 3.5PN order [17].

The TaylorT4 waveforms used here are computed in the so-called “restricted” amplitude approximation, which assumes the waveform amplitude to be zeroth post-Newtonian order and only includes the leading second harmonic of the orbital phase. We only include the leading second harmonic of the orbital phase in the EOBNR waveforms. We do not consider the effects of spin or eccentricity in any of the waveform families, as we restrict to circular orbits and non-spinning black holes.

The HG and TaylorT4 families are inspiral-only time-domain waveforms and are terminated when the gravitational waveforms reach the ISCO frequency.

III. SNR FROM INSPIRAL, MERGER AND RINGDOWN

In this section we consider the relative contributions of the different portions of the gravitational-wave coalescence signal to the SNR as a function of the IMRAC’s mass.

We work in the frequency domain and define the Fourier transform of the gravitational-wave strain signal, $\tilde{h}(f)$, as

$$\tilde{h}(f) = \int_{-\infty}^{+\infty} dt h(t) e^{-2\pi i f t}, \quad (3.1)$$

where $h(t)$ is the time-domain strain signal. We define the noise-weighted inner product as

$$(a|b) = 4\Re \left[\int_{f_{\min}}^{f_{\max}} df \frac{\tilde{a}(f)\tilde{b}^*(f)}{S_n(f)} \right], \quad (3.2)$$

where $S_n(f)$ is the instrument noise power spectral density (PSD), which we will take to be the Advanced LIGO high-power, zero-detuned noise PSD [20]. The limits of integration correspond to the bandwidth of the detector. The expectation value of the optimal matched filtering SNR, in the case when the signal and template waveforms are identical, is given by [21]

$$\begin{aligned} \left(\frac{S}{N}\right)_{\max} &= (h|h)^{1/2}, \\ &= \left[4\Re \int \left(\frac{f|\tilde{h}(f)|}{\sqrt{fS_n(f)}} \right)^2 d \ln f \right]^{1/2}. \end{aligned} \quad (3.3)$$

Writing the maximum SNR in the form above clearly separates it into contributions from the signal strain, $f|\tilde{h}(f)|$, and the root-mean-squared (rms) noise spectral amplitude, $\sqrt{fS_n(f)}$, which is the strain signal associated with the detector noise.

One can gain insight into the relative contributions to the SNR from inspiral, merger and ringdown by comparing the gravitational-wave strain to the noise rms value. In Fig. 1 we show the strain for selected overhead and face-on (i.e., optimally-located and oriented) IMRAC sources at a fiducial distance of 1Gpc as described by the

EOBNR waveform family, and noise rms amplitude. The ISCO frequency of each signal is shown as a vertical line. The strain from merger and ringdown is thus the portion after the ISCO frequency. The contribution to the strain from merger and ringdown from binaries with component masses $(m_1, m_2) = [(200, 20) M_\odot, (200, 2) M_\odot]$, is greater than that of the noise rms amplitude (black curve with triangles). In general, systems with ISCO frequencies between 30 – 100 Hz, merge in the “bucket” of the noise curve, i.e., where the detector is most sensitive. For example, for the $(m_1, m_2) = (200, 20) M_\odot$ system (red dotted curve in Fig. 1), the merger and ringdown contribute the bulk of the SNR. Conversely, the inspiral contribution to the SNR is strongly suppressed for such massive systems.

In Fig. 2 we show the maximum SNR, Eq. (3.3), as a function of the binary’s total mass produced by inspiral-only and full EOBNR waveforms at four different mass-ratios in the range $1/200 \leq q \leq 1/10$. We construct inspiral-only EOBNR waveforms by Fourier transforming the full waveform into the frequency domain and truncating it at the ISCO frequency. We have considered the SNR for optimally-located and oriented sources at a fiducial distance of 1 Gpc. The lower-bound mass of the smaller body is set to $m_2 = 1.4 M_\odot$ which is the canonical neutron-star mass. The lowest total mass for the $q = 1/50$, $1/100$ and $1/200$ subplots is set by fixing the mass of the smaller body to $m_2 = 1.4 M_\odot$. For the $q = 1/10$ subplot in Fig. 2 the smallest total mass is set to $M = 35 M_\odot$ as the inspiral phase accounts for the vast majority of the SNR below this value. The lower limit of integration of Eq. (3.3) is 10 Hz and the upper limit is 2048 Hz, which is the Nyquist frequency of discretely sampled EOBNR waveforms generated at a sampling rate of $\Delta t = 4096$ s in the time-domain. We only consider systems with total masses such that the ISCO frequency is greater than 10 Hz (our low frequency cut-off). The highest total mass for each of the subplots in Fig 2 is set to $M = 300 M_\odot$ which ensures the ISCO frequency is greater than 10 Hz.

As anticipated from Fig. 1 there is a significant difference in the SNR between inspiral-only and full EOBNR waveforms that can be seen at all four mass ratios. We also note that for systems with mass ratios of $q = 1/10$ with total masses below around $M = 35 M_\odot$ the inspiral phase is the dominant source of SNR. If we consider 3% as a fiducial value of the difference between the full SNR and the one associated to the inspiral-only waveform – which leads to a loss in detection rates of 10% – this happens at $M \approx 35 M_\odot$ for $q = 1/10$. For binaries with $q = 1/50$, $1/100$ and $1/200$, the minimum difference in SNR between inspiral-only and full waveforms is $\approx 6\%$, 15% and 40% respectively for the mass ranges considered in Fig 2.

In summary, we have shown that inspiral-only templates will miss a significant portion of the total SNR of IMRAC signals over the bulk of the detectable mass-space. Future searches will therefore require templates

that can match the full inspiral-merger-ringdown. However, there is a small region of the parameter space for which inspiral-only templates may suffice for searches, without inducing drastic losses in detection rates. In the following section we quantify the effectiveness of inspiral-only templates for searching for full coalescence signals in aLIGO.

IV. EFFECTIVENESS OF INSPIRAL-ONLY TEMPLATES FOR IMRAC SEARCHES

We have shown in Sec. III that the SNR from merger and ringdown will provide a significant contribution to the total SNR over a broad portion of the IMRAC mass-space, c.f. Fig. 2. There is however a small portion of the parameter space where the SNR is dominated by the inspiral phase. This can be seen in Fig. 2 for binaries with $q = 1/10$ binaries in Fig. 2 with total masses $M \leq 35 M_\odot$. Thus it is important to quantify the effect of using inspiral-only templates to search for IMRAC signals which contain inspiral, merger and ringdown phases. The use of template waveforms that are not exact representations of the signals they filter degrades the SNR, as the optimal SNR can be recovered only when the template waveform corresponds exactly to h , see Eq. (3.3). In practice however, we do not have access to an exact representation for h . Using a non-exact template waveform T to filter h caps the maximum recoverable SNR to

$$\begin{aligned} \left(\frac{S}{N}\right) &= \max_{\vec{\theta}} \frac{(h(\vec{\lambda})|T(\vec{\theta}))}{(T(\vec{\theta})|T(\vec{\theta}))^{1/2}}, \\ &= \epsilon \left(\frac{S}{N}\right)_{max}, \end{aligned} \quad (4.1)$$

where $\vec{\lambda}$ and $\vec{\theta}$ represent the parameter vector of the signal and template, respectively. We define ϵ as the *effectiveness* of a template waveform family T at recovering the maximum SNR from a gravitational-wave signal h ; by definition $0 \leq \epsilon \leq 1$. This quantity is also referred to as the “fitting factor” in the literature [22]. It is convenient to define waveforms normalized to unit norm as $\hat{\mathbf{a}}(f) = \tilde{a}(f)/(a|a|)^{1/2}$ so that $(\hat{\mathbf{h}}|\hat{\mathbf{h}}) = (\hat{\mathbf{T}}|\hat{\mathbf{T}}) = 1$ and the effectiveness can be written succinctly as [22]

$$\epsilon = \max_{\vec{\theta}} (\hat{\mathbf{h}}(\vec{\lambda})|\hat{\mathbf{T}}(\vec{\theta})). \quad (4.2)$$

Using normalized waveforms also has the advantage of eliminating the dependence of the waveforms on the source orientation and distance, which enter as an overall scaling.

Calculating the effectiveness, Eq. (4.2), requires maximizing over the component masses (m_1, m_2) and the time and phase at coalescence. We can efficiently maximize over the time and phase by Fourier transforming the integrand of the noise-weighted inner-product [23],

$$z(t_c) = 4 \int_{f_{min}}^{f_{max}} df \frac{\tilde{a}(f)\tilde{b}^*(f)}{S_n(f)} e^{2\pi i f t_c}, \quad (4.3)$$

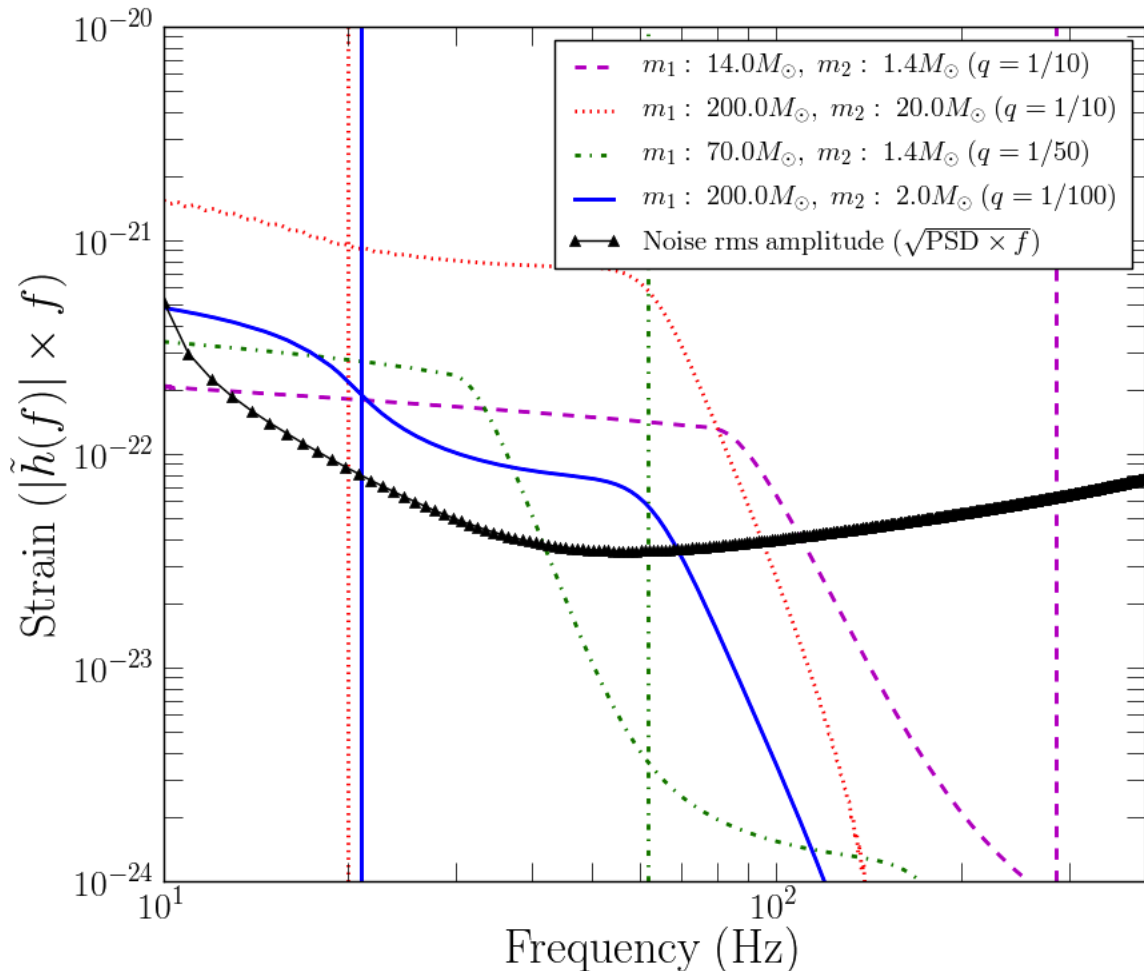


FIG. 1: Strain of optimally-located and oriented IMRAC sources at a fiducial distance of 1 Gpc as described by EOBNR waveforms, and aLIGO noise. The corresponding ISCO frequency of each signal is shown as a vertical line. The strain from the merger and ringdown from each source contributes after the ISCO frequency. For the sources with component masses $(m_1, m_2) = [(200, 20) M_\odot, (200, 2) M_\odot]$, the strain from merger and ringdown sits above the noise spectrum. The SNR from the full EOBNR waveform and from its inspiral-only portion are shown in Fig. 2.

which yields a complex time series whose elements correspond to the inner-product of a and b as one of the signals is time-shifted with respect to the other. We can efficiently find the time at coalescence, t_c , by finding the time at which the norm of this time series is a maximum. The phase at coalescence ϕ_c is then automatically given by finding the argument of the time-series at its peak amplitude. We thus modify the inner product $(a|b)$:

$$(a|b) \rightarrow (a|b)' = \max_{t_c} |z(t_c)|, \quad (4.4)$$

which we will adopt as the definition of the inner-product for the remainder of this paper.

To compute the effectiveness of an inspiral-only IMRAC search we evaluate Eq. (4.2) for signals covering the IMRAC mass space. We take as our signal waveform, h , the full inspiral-merger-ringdown EOBNR waveform. We take the template, T , to be an *inspiral-only* EOBNR waveform, formed by truncating the full EOBNR wave-

form at the ISCO frequency in the frequency domain. With such signals and templates the effectiveness provides a measure of the maximum SNR which could be achieved through using an inspiral-only template to filter full coalescence-signals. To get a broad coverage of the IMRAC mass space we compute Eq. (4.2) for signals whose source masses cover the ranges $1.4 M_\odot \leq m_2 \leq 18.5 M_\odot$ and $24 M_\odot \leq m_1 \leq 200 M_\odot$, with mass ratios spanning the range $q := m_2/m_1 \in [1/140, 1/10]$. For each signal we evaluate the effectiveness, Eq. (4.2), where the template T describes the inspiral-only portion of an EOBNR waveform. We maximize over time and phase by maximizing the inner product of the signal with an inspiral-only EOBNR template, Eq. (4.4). The maximization over the masses is performed by finding the largest inner product between the signal and a bank of template waveforms. The template bank is characterised by intrinsic parameters (\mathcal{M}, η) which are

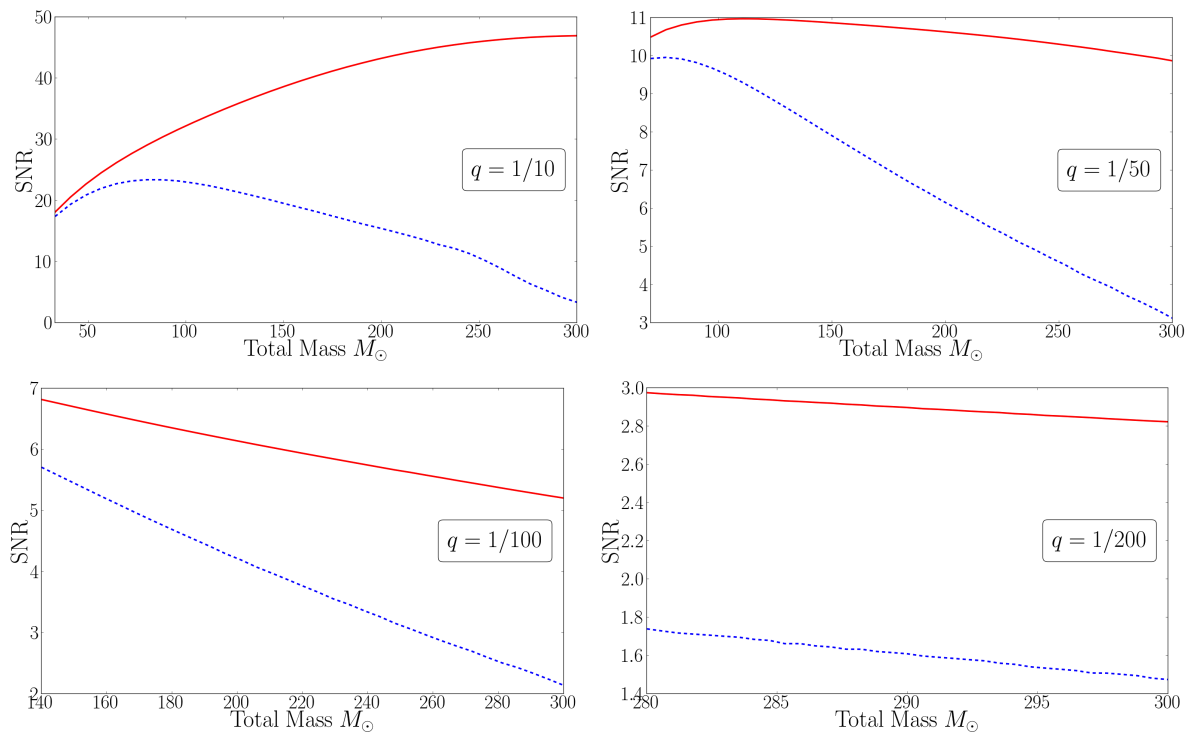


FIG. 2: SNR of optimally-located and oriented IMRAC sources at a fiducial distance of 1 Gpc vs total mass for four different mass ratios; $q = 1/10, 1/50, 1/100, 1/200$. The solid line is the SNR from full EOBNR waveforms and the dashed line from inspiral-only EOBNR waveforms truncated at the ISCO frequency in the frequency domain. The lower-bound mass of the smaller body is set to $m_2 = 1.4 M_\odot$ which is the canonical neutron-star mass. The lowest total mass for the $q = 1/50, 1/100$ and $1/200$ subplots in Fig. 2 is set by fixing the mass of the smaller body to $m_2 = 1.4 M_\odot$. For the $q = 1/10$ subplot the smallest total mass is set to $M = 35 M_\odot$ as the inspiral accounts for the vast majority of the SNR below this value. We only consider systems with total masses such that the ISCO frequency is greater than 10 Hz (our low frequency cut-off). The highest total mass for each of the subplots in Fig 2 is set to $M = 300 M_\odot$ which ensures that the ISCO frequency is greater than 10 Hz. We find that there is a non-negligible contribution to the SNR from merger and ringdown in IMRAC signals above a total mass of around $M = 35 M_\odot$. The difference in SNR between inspiral-only and full waveforms is at the 3% level at around $M = 35 M_\odot$ at $q = 1/10$. For binaries with $q = 1/50, 1/100$ and $1/200$, the minimum loss in SNR are at the 6%, 15% and 40% levels, respectively, in our mass range of interest. For IMRACs of astrophysical interest, more extreme mass ratios correspond to greater total mass, which can place the merger and ringdown at a frequency where the detector has the greatest sensitivity.

the chirp mass and symmetric mass ratio of the system: $\mathcal{M} = (m_1 m_2)^{3/5} / (m_1 + m_2)^{1/5}$, $\eta = (m_1 m_2) / (m_1 + m_2)^2$, where m_1 and m_2 are the component masses of the binary. The bank spans an extended mass range $3 M_\odot \leq \mathcal{M} \leq 30 M_\odot$ and $0.0065 \leq \eta \leq 0.082$. The results of the effectiveness of an inspiral-only IMRAC search are shown in Fig. 3.

Inspiral-only templates are $\sim 98\%$ effective at filtering full coalescence signals for total masses $M \lesssim 30 M_\odot$. Such systems have an ISCO frequency $150 \text{ Hz} \lesssim f_{\text{ISCO}}$ which is well within the peak sensitivity of the noise curve. However for the bulk of the mass space the effectiveness is below 75%. This is unsurprising given the SNR curves in Fig. 2 which clearly show the importance of the contribution of merger and ringdown to the SNR.

The loss in SNR incurred through using inspiral-only templates directly affects detection rates. Because the SNR scales inversely with the distance, the observable volume will scale with the cube of the effectiveness. As-

suming that GW sources are isotropically distributed in the sky, the fractional loss in detection rates will be $L = 1 - \epsilon^3$, assuming that detectability is determined by SNR threshold alone. The percentage loss in detection rates through using inspiral-only EOBNR templates to recover the full coalescence signal is also shown in Fig. 3. Over a broad portion of the mass-space inspiral-only templates incur losses in detection rates between 60 – 85%. As the total mass of the binary approaches $440 M_\odot$ the Schwarzschild ISCO frequency, Eq. (1.1), approaches 10 Hz which is near the low-frequency cut-off of the detectors. Hence the relative contribution of the inspiral phase to the coalescence signal of heavier systems diminishes until the only contribution is from the merger and ringdown. This is a striking indication of the need of merger and ringdown in IMRAC template waveforms. This suggests the importance of full numerical simulations in this regime in order to construct a reliable waveform family including inspiral, merger, and

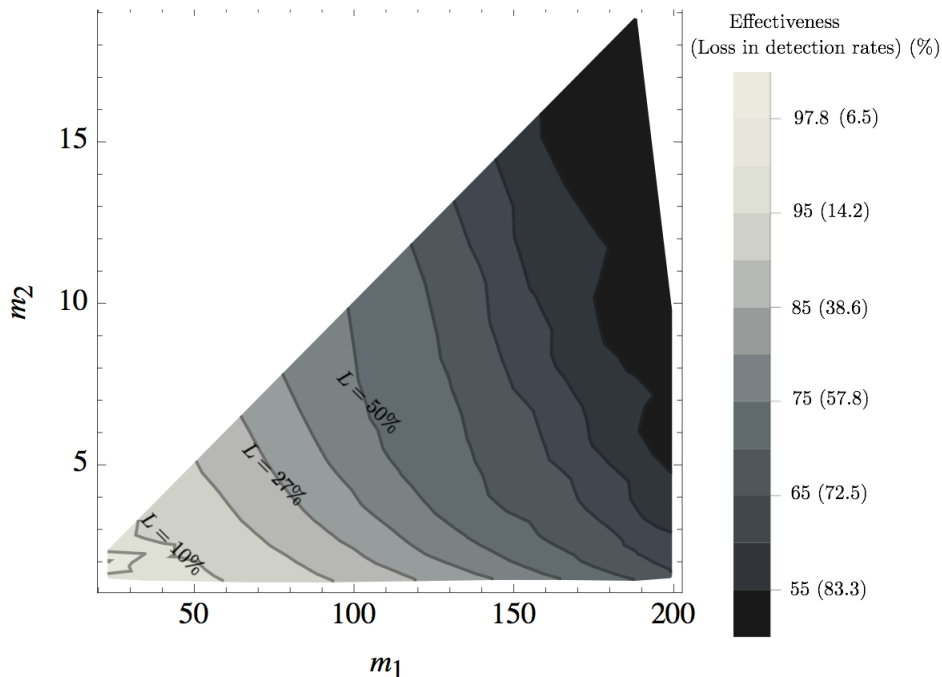


FIG. 3: Effectiveness of inspiral-only EOBNR templates to filter full inspiral, merger and ringdown EOBNR signals as a function of the source component masses and corresponding loss in detection rates. The diagonal corresponds to a mass ratio $q = 1/10$. Inspiral-only EOBNR templates are constructed by truncating the full waveform at the ISCO frequency in the frequency-domain. For the bulk of the parameter space inspiral-only templates are $\lesssim 75\%$ effective at filtering inspiral, merger and ringdown signals. Inspiral-only templates are $\sim 97 - 98\%$ effective for total masses $M_{\odot} \lesssim 30 M_{\odot}$. Inspiral-only templates within the 90%-effectiveness contour should be sufficient for IMRAC searches without incurring greater than 30% losses in detection rates. The contours corresponding to losses in detection rates $L = 10\%$, $L = 27\%$ and $L = 50\%$ have been highlighted.

ringdown phases.

We identify three regions in the m_1 - m_2 plane in which various searches could be constructed. The regions are defined by contours of constant effectiveness which are approximately given by $\mathcal{C} = (m_1/M_{\odot})\sqrt{m_2/M_{\odot}}$, which are found purely empirically, with $1.4 M_{\odot} \leq m_2 \leq 18.5 M_{\odot}$ and mass ratios $q \in [1/140, 1/10]$. The effectiveness is related to \mathcal{C} by $\epsilon \approx 1/100 \times (1.6 \mathcal{C} - 7.3 \times 10^{-3} \mathcal{C}^2)$.

Between the 97%- and 90%-effectiveness contours, the losses in detection rates are between $10\% \lesssim L \lesssim 27\%$ and so an inspiral-only search could be sufficient without incurring drastic losses in detections. The region bound from below in effectiveness by the 90%-effectiveness contour is defined by $\mathcal{C} \leq 100$, with the effectiveness increasing with decreasing \mathcal{C} . Between the 90%- and 80%-effectiveness contours the losses in detection rates are around $27\% \lesssim L \lesssim 50\%$. Thus, within this region searches will be limited by the lack of merger and ringdown in template waveforms, though an inspiral-only search would be feasible in principle. This contour is defined by $100 \lesssim \mathcal{C} \lesssim 150$. Below the 80%-effectiveness contour, inspiral-only searches will incur losses in detection $50\% < L$ and so merger and ringdown will be crucial for searches. The region bound from above in effectiveness by the 80%-effectiveness contour which is defined by $150 \lesssim \mathcal{C}$, with effectiveness decreasing with increasing

\mathcal{C} . The results are summarized in Table I. We note that these contours are accurate to within around 5% of the true value of the constant-effectiveness contours between the $L = 10\%$ and $L = 50\%$ contours. Below the $L = 10\%$ and beyond the $L = 50\%$ contours the accuracy deteriorates, however we do not consider individual contours outside these ranges.

A. Bias in parameter estimates from inspiral-only waveforms

The parameters of the binary are encoded in the gravitational-wave signal. The template gravitational waveform which maximises the SNR yields the best-fit estimate of the binary's parameters. Neglecting the merger and ringdown in template waveforms can lead to biases in the best-fit parameters when the signal describes the full inspiral, merger and ringdown phases of coalescence. Here, we analyze biases in the mass parameters: the chirp mass \mathcal{M} and the symmetric mass ratio η .

In Fig. 4 we compare biases in the best-fit values of chirp mass and symmetric mass ratio obtained with inspiral-only template waveforms as a function of the chirp mass encoded in full EOBNR signal waveforms. We report the fractional bias in the chirp mass and

Effectiveness of inspiral-only search, $\epsilon(\%)$	Loss in detection rates, $L(\%)$	Contours of constant effectiveness in m_1 - m_2 plane ($\mathcal{C} = (m_1/M_\odot)\sqrt{m_2/M_\odot}$) within mass range of interest	Implication for searches
$90\% \lesssim \epsilon \lesssim 97\%$	$10\% \lesssim L \lesssim 27\%$	$\mathcal{C} \lesssim 100$	Inspiral-only search sufficient but with non-negligible loss in detection rates.
$80\% \lesssim \epsilon \lesssim 90\%$	$27\% \lesssim L \lesssim 50\%$	$100 \lesssim \mathcal{C} \lesssim 150$	Inspiral-only search possible but limited by lack of merger and ringdown. Could potentially lose half of signals with inspiral-only templates.
$\epsilon \lesssim 80\%$	$50\% \lesssim L$	$150 \lesssim \mathcal{C}$	Merger and ringdown crucial for searches. Will miss over half of signals with inspiral-only templates.

TABLE I: Effectiveness of inspiral-only searches, the corresponding loss in detection rates and the region in the m_1 - m_2 plane bounded by constant-effectiveness contours. For a given region in the m_1 - m_2 plane bounded by constant-effectiveness contours we summarize the implications for IMRAC searches.

mass ratio: $\Delta\mathcal{M}/\mathcal{M} = (\mathcal{M}^{\text{best fit}} - \mathcal{M}^{\text{true}})/\mathcal{M}^{\text{true}}$ and $\Delta\eta/\eta = (\eta^{\text{best fit}} - \eta^{\text{true}})/\eta^{\text{true}}$.

These systematic biases should be compared against typical statistical measurement uncertainties. However, approximate techniques for estimating measurement uncertainty from the Fisher information matrix are notoriously unreliable [24, 25], and a full Bayesian treatment of IMRAC parameter estimation is beyond the scope of this paper. We note, however, that for comparable-mass binaries, the chirp mass and symmetric mass ratio can typically be measured to within $\mathcal{O}(1\%)$ and $\mathcal{O}(10\%)$ of the signal value [26].

For the $q = 1/10$ and $q = 1/20$ cases we find that biases in the best-fit parameters can be as low as $\Delta\mathcal{M}/\mathcal{M} \sim 0.1\%$ and $0.1\% \lesssim \Delta\eta/\eta \lesssim 10\%$ for values of the signal chirp mass $\mathcal{M} \lesssim 15 M_\odot$. These biases are lower than typical measurement uncertainty. However, the biases in chirp mass and symmetric mass ratio rise significantly for $\mathcal{M} \gtrsim 15 M_\odot$ for the $q = 1/10$ and $q = 1/20$ cases: the biases in chirp mass can be as high as 20% and 30% respectively, and those for symmetric mass ratio as high as 120% and 160% respectively. Such high errors are due to the increased importance of merger and ringdown in the signal waveform at higher chirp mass.

For the $q = 1/55$ case we find similar behaviour in the bias in best-fit chirp mass and symmetric mass ratio, although the smallest biases in symmetric mass ratio are of the order of $\Delta\eta/\eta \sim 10\%$ for masses in the range of interest. In addition, we find that the bias in chirp mass is on the order of $\Delta\mathcal{M}/\mathcal{M} \sim 0.1\%$ for chirp mass signal values in the range $7 M_\odot \lesssim \mathcal{M} \lesssim 10 M_\odot$. However, the biases grow rapidly to 40% when the signal value of chirp mass exceeds $10 M_\odot$. For the $q = 1/100$ case we find that the smallest bias in chirp mass and symmetric mass ratio are around 4% and 20% respectively.

These results suggest that inspiral-only waveforms may only be able to provide faithful estimates of the binary's

masses in some limited cases. For high-mass systems, the best-fit mass parameter estimates are likely to be highly unreliable.

V. COMPARISON OF INSPIRAL-ONLY WAVEFORMS

We have shown that merger and ringdown are crucial for effective searches over a large portion of the IMRAC mass space, though there is a small region in which an inspiral-only search could be constructed without incurring losses in detection rates greater than around 27%. For this region, it is therefore important to study whether currently available waveforms are sufficiently accurate. The inspiral phase can be computed using perturbative expansions and thus it is interesting to quantify the consistency of different expansions.

To assess the effectiveness of the EOBNR inspiral, we employ a waveform family designed to approximate intermediate mass-ratio inspirals which we refer to as ‘‘Huerta-Gair’’ (HG) waveforms [16]. HG waveforms describe only the inspiral portion of the coalescence signal. This waveform family has no corresponding LAL approximant.

We repeat the study done in the previous Section using now the HG waveform family as the signal h and inspiral-only EOBNR as the template T . The results are reported over the whole parameter space in Fig. 5. For completeness, in Table II we also show the values of the effectiveness, Eq. 4.2, for selected mass combinations of EOBNR inspiral-only templates for filtering full EOBNR and HG signals respectively.

For the high-mass part of the mass-space the effectiveness of the EOBNR inspirals with respect to the HG waveforms is close to 100%. This is perhaps unsurprising because very high mass systems will have short inspi-

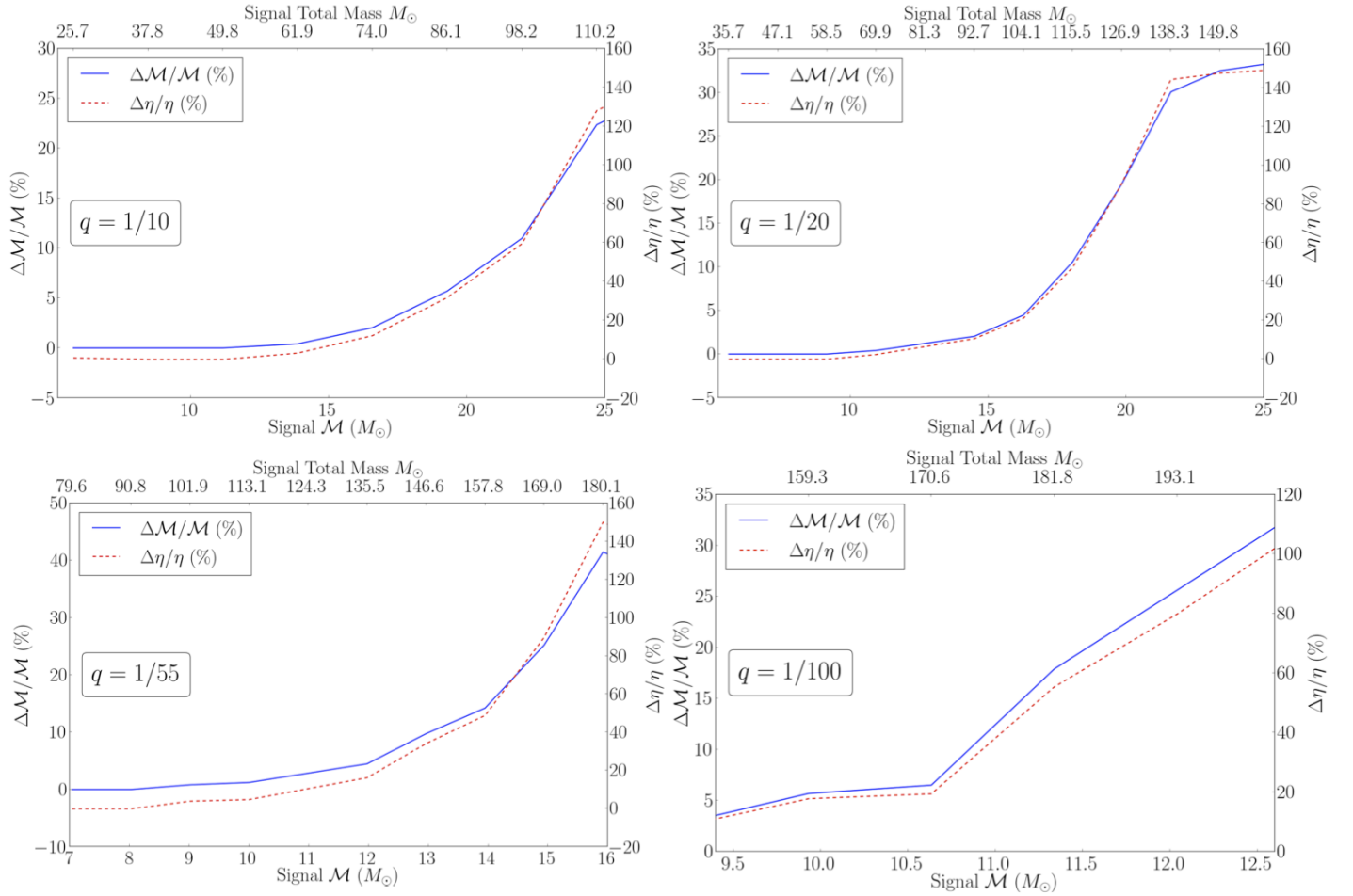


FIG. 4: Biases in best-fit estimates, incurred through using inspiral-only template waveforms, of chirp mass \mathcal{M} and symmetric mass ratio η as a function of chirp mass of a signal waveform that describes the inspiral, merger and ringdown phases of coalescence. Biases are shown for four different mass ratios of the signal waveform, $q = 1/10, 1/20, 1/55, 1/100$. The biases $\Delta\mathcal{M}/\mathcal{M}$ and $\Delta\eta/\eta$ are measured as the ratio of the difference between the best-fit and the signal parameter to the signal parameter: $\Delta\mathcal{M}/\mathcal{M} = (\mathcal{M}^{\text{best fit}} - \mathcal{M})/\mathcal{M}$ and $\Delta\eta/\eta = (\eta^{\text{best fit}} - \eta)/\eta$. For convenience we have also shown the total mass of the signal on the upper x-axis.

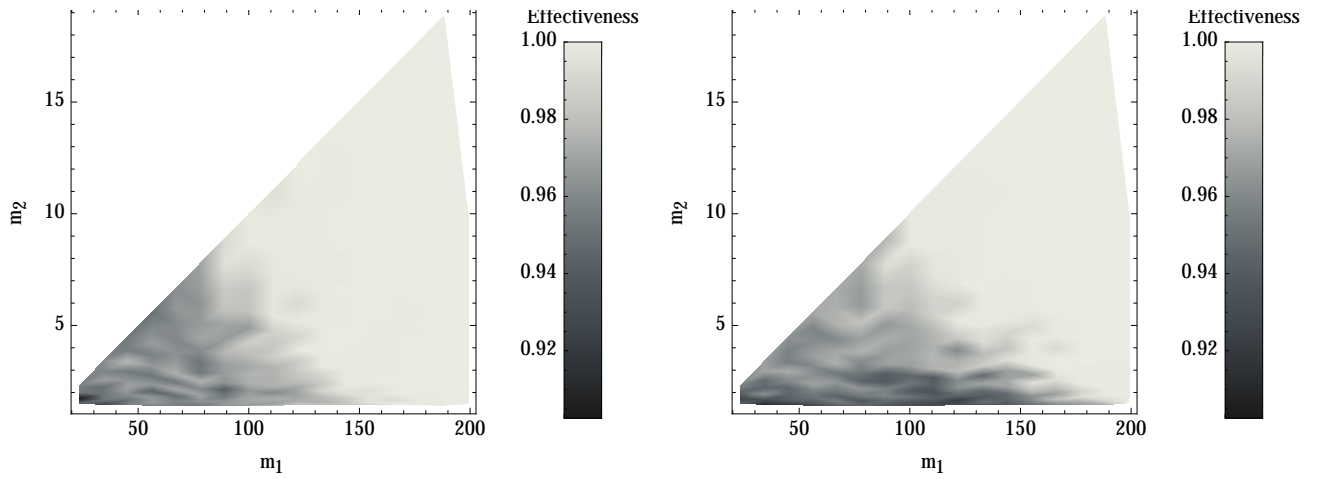


FIG. 5: Effectiveness of inspiral-only EOBNR templates at filtering HG signals (left) and TaylorT4 signals (right) as a function of the source component masses encoded in the signal.

m_1 (M_\odot)	m_2 (M_\odot)	Signal waveforms		
		full EOBNR	Huerta-Gair	TaylorT4
50	5	0.90	0.95	0.96
100	5	0.76	0.97	0.97
200	5	0.53	0.99	0.99
50	1.4	0.96	0.96	0.90
100	1.4	0.86	0.98	0.94
200	1.4	0.67	0.98	0.98

TABLE II: Summary of effectiveness of *inspiral-only* EOBNR template waveforms in recovering signals modelled using different waveform families – full EOBNR, Huerta-Gair and TaylorT4 – for selected component masses. Merger and ringdown become more prominent in the coalescence signal as the total-mass of the system is increased. The EOBNR inspiral is typically better at matching HG signals in the IMRAC regime than TaylorT4 signals.

rals and possible differences in the waveforms will not produce a significant degradation of SNR when matched over a small number of wave cycles. However, for lighter systems the effectiveness can be as low as 90%, which occurs in the region of mass space in which inspiral-only searches would be most feasible (see Table I).

For reference we also compare inspiral-only EOBNR templates to TaylorT4 [16] signal waveforms (which are inspiral-only). We construct signal waveforms on the same grid in $m_1 - m_2$ as for HG waveforms and use the same template bank of inspiral-only EOBNR waveforms. The results are summarized in the right panel of Fig. 5, and in Table II for selected masses. We find that the EOBNR inspiral has good filtering efficiency for the TaylorT4 waveform family. However, EOBNR is clearly a better match to the HG waveform family over a larger range of masses and mass ratios than to TaylorT4. This can be seen more clearly by comparing the subplots in Fig. 5. This is unsurprising given that the PN expansion is unreliable at high velocities and highly asymmetrical mass ratios. For orbital velocities $v/c = (M\pi f)^{1/3} \gtrsim 0.2$ the PN energy flux deviates significantly from numerical results, see [e.g., 27, 28]. A binary at its ISCO frequency has $v/c \sim 0.4$, which is well beyond the region of validity.

VI. DISCUSSION AND CONCLUSION

We have shown that over the bulk of the IMRAC mass space, merger and ringdown contribute significantly to the gravitational-wave coalescence signal. This happens despite the suppression of the power in the merger and ringdown in signals from binaries with very asymmetric mass ratios. The importance of merger and ringdown is due to the greater sensitivity to these waveform portions for high-mass signals, for which most of the inspiral may fall at frequencies below the detector’s sensitive band.

However there is a relatively large patch in mass space in which the inspiral-only waveforms are more than 90% effective. We identified three regions in which different searches could be considered appropriate based on thresholds of acceptable losses in detection rates. The mass space splits into a region in which inspiral-only searches could be feasible, incurring losses in detection rates of up to $\sim 27\%$; a region in which searches would be limited by lack of merger and ringdown in template waveforms, incurring losses in detection rates up to 50%; and a region in which merger and ringdown are critical to prevent losses in detection rates over 50%. The search regions are summarized in Table I.

We have further shown that in the region of the IMRAC mass space in which inspiral-only searches are feasible, approximants adapted to asymmetric mass-ratio binaries are important, as here the binary is liable to have highly relativistic velocities $v/c \gtrsim 0.2$. We considered a waveform family designed to describe intermediate mass-ratio binaries which we referred to as the “Huerta-Gair” (HG) waveform family. By computing the effectiveness of inspiral-only EOBNR waveforms to filter signals described by the HG waveform family, we showed that losses in recovered SNR could be as great as 10%. In Table II we summarize the effectiveness of the signal-template combinations used in the paper.

We believe that template waveforms for IMRAC searches will benefit from calibration to several numerical simulations. We note that there already exists one very short numerical waveform of a $q = 1/100$ binary which we have not used in our study, and which EOBNR is not currently calibrated to [12].

In addition, it would be interesting to extend the study performed here to the case of binaries in which the components are spinning. The presence of spin in a binary leads to modulations in the emitted gravitational waveform’s phase and amplitude [22]. Using template waveforms which do not account for the presence of spins can lead to further reductions in SNR [29] and systematic biases in parameter estimation, as the template waveforms will fail to account for the correct phasing of the signal waveform contained in data.

VII. ACKNOWLEDGEMENTS

We thank Jonathan Gair for useful discussions and help in implementing the HG waveform family and Chad Hanna for useful discussions. We would also like to thank Elio Antonio Huerta Escudero for reading a draft of the manuscript and providing us with useful comments. Research at Perimeter Institute is supported through Industry Canada and by the Province of Ontario through the Ministry of Research & Innovation. This document has LIGO document number ligo-p1300009.

-
- [1] M. C. Miller, *Class. Quant. Grav.* **26**, 094031 (2009).
- [2] M. C. Miller and E. J. M. Colbert, *Int. J. Mod. Phys. D* **13**, 1 (2004).
- [3] G. Harry and The LIGO Scientific Collaboration, *Class. Quant. Grav.* **27**, 084006 (2010).
- [4] The Virgo Collaboration, *Advanced virgo baseline design note vir027a0* (2009), URL <https://tds.ego-gw.it/itf/tds/file.php?callFile=VIR-0027A-09.pdf>.
- [5] K. Somiya, *Classical and Quantum Gravity* **29**, 124007 (2012).
- [6] J. Abadie and The LIGO Scientific Collaboration, *Class. Quant. Grav.* **27**, 173001 (2010).
- [7] D. A. Brown, J. Brink, H. Fang, J. R. Gair, C. Li, G. Lovelace, I. Mandel, and K. S. Thorne, *Phys. Rev. Lett.* **99**, 201102 (2007).
- [8] I. Mandel, D. A. Brown, J. R. Gair, and M. C. Miller, *Astrophys. J.* **681**, 1431 (2008).
- [9] C. L. Rodriguez, I. Mandel, and J. R. Gair, *Phys. Rev. D* **85**, 062002 (2012).
- [10] C. O. Lousto, H. Nakano, Y. Zlochower, and M. Campanelli, *Phys. Rev. D* **82**, 104057 (2010).
- [11] Y. Pan, A. Buonanno, M. Boyle, L. T. Buchman, L. E. Kidder, H. P. Pfeiffer, and M. A. Scheel, *Phys. Rev. D* **84**, 124052 (2011).
- [12] H. Nakano, Y. Zlochower, C. O. Lousto, and M. Campanelli, *Phys. Rev. D* **84**, 124006 (2011).
- [13] J. R. Gair and K. Glampedakis, *Phys. Rev. D* **73**, 064037 (2006).
- [14] S. Babak, H. Fang, J. R. Gair, K. Glampedakis, and S. A. Hughes, *Phys. Rev. D* **75**, 024005 (2007).
- [15] E. A. Huerta and J. R. Gair, *Phys. Rev. D* **79**, 084021 (2009).
- [16] E. Huerta and J. R. Gair, *Phys. Rev. D* **83**, 044020 (2011).
- [17] A. Buonanno, B. R. Iyer, E. Ochsner, Y. Pan, and B. S. Sathyaprakash, *Phys. Rev. D* **80**, 084043 (2009).
- [18] I. Mandel and J. R. Gair, *Class. Quant. Grav.* **26**, 094036 (2009).
- [19] The LIGO Scientific Collaboration, arXiv:1209.6533 (2012).
- [20] The LIGO Scientific Collaboration, *Tech. rep. ligo-t0900288-v3 ligo project* (2009), URL https://dcc.ligo.org/DocDB/0002/T0900288/003/AdvLIGO_noise_curves.pdf.
- [21] C. Cutler and E. Flanagan, *Phys. Rev. D* **49**, 2658 (1994).
- [22] T. A. Apostolatos, *Phys. Rev. D* **52**, 605 (1995).
- [23] B. Allen, W. G. Anderson, P. R. Brady, D. A. Brown, and J. D. E. Creighton, *Phys. Rev. D* **85**, 122006 (2012).
- [24] M. Vallisneri, *Phys. Rev. D* **77**, 042001 (2008).
- [25] M. Vallisneri, *Phys. Rev. Lett.* **107**, 191104 (2011).
- [26] J. Aasi and The LIGO Scientific Collaboration and The Virgo Collaboration, arXiv:1304.1775 (2013).
- [27] E. Poisson, *Phys. Rev. D* **52**, 5719 (1995).
- [28] N. Yunes and E. Berti, *Phys. Rev. D* **77**, 124006 (2008).
- [29] P. Ajith, N. Fotopoulos, S. Privitera, A. Neunzert, and A. J. Weinstein, arXiv:1210.6666 (2012).